Journal of South American Earth Sciences 74 (2017) 27–40

Contents lists available at ScienceDirect

Journal of South American Earth Sciences

journal homepage: www.elsevier.com/locate/jsames

Architecture of the intracontinental Jaibaras Rift, Brazil, based on geophysical data

Nilo C. Pedrosa Jr. [a, b, c, *], Roberta M. Vidotti [b], Reinhardt A. Fuck [b], R.M.G. Castelo Branco [d], Afonso R. de Almeida [d], Nilton C. Vieira Silva [d], Luiz R.C. Braga [d]

[a] Graduate Program in Regional Geology, Universidade de Brasília, Brazil
[b] Instituto de Geociências, Universidade de Brasília, Campus Universitário Darcy Ribeiro ICC - Ala Central, CEP 70910-900 Brasília, Brazil
[c] Geological Survey of Brazil, Rua Goiás, 312, CEP 64001-570 Teresina, Brazil
[d] Universidade Federal do Ceará, Campus Universitário do PICI 1011, CEP 60455-760 Fortaleza, Brazil

ARTICLE INFO

Article history:
Received 16 September 2016
Received in revised form
29 December 2016
Accepted 29 December 2016
Available online 31 December 2016

Keywords:
Potential methods
Magnetotelluric data
Magnetic-gravity 2D joint modeling
Rift geometry and evolution
Jaibaras Rift

ABSTRACT

Qualitative and quantitative integration and interpretation of magnetic, gravity and magnetotelluric data help to determine the internal architecture of the Jaibaras rift, and allow assessing the evolution of the Jaibaras Rift within the Precambrian crystalline basement of Borborema Province, NE Brazil. This was achieved by 2D joint modeling of magnetic and gravity data in five sections across the main axis of the Jaibaras Rift. Surface data, rock density measurements, depth constraints from 2D Euler deconvolution and geophysical information from previous work in the area were integrated to constrain the modeling. The magnetic and gravity profiles of the Jaibaras Rift indicate estimated source bodies at depths up to 2.5 km, showing complex configuration for the structural framework, with a set of asymmetric grabens and horsts. The 2D magnetotelluric inversion shows that the Jaibaras Rift is marked by low resistivity values, and maximum thickness of the sedimentary package up to approximately 3 km. Shallow dipping conductive material may represent either a suture zone between the Ceará Central and Médio Coreaú domains or a set of fractures due to horizontal σ_1 stress in the Ceará Central Domain. The Jaibaras Rift displays a very complex internal structure, with discontinuous sequences of grabens and horsts, and a significant volume of surface and subsurface volcanic rocks. The sedimentary packages with volcanic rift sequences have variable thicknesses, from 1 to 3 km. These rock units are controlled by normal faults that developed from older discontinuities, such as the Transbrasiliano lineament.

1. Introduction

The Jaibaras Rift is located at the boundary between the Ceará Central (CCD) and Médio Coreaú (MCD) domains, in the northern portion of the Borborema Province, northeast Brazil (Fig. 1). The rift is characterized by a NE-SW trending axis, and it is about 120 km long and 3–15 km wide (Fig. 2). The rift occurs along the northern part of the Transbrasiliano Lineament (Schobbenhaus et al., 1975), locally known as Sobral-Pedro II Shear Zone (SPIISZ), with dextral strike-slip kinematics (Almeida, 1998; Oliveira, 2001; Oliveira and Mohriak, 2003; Pedrosa et al., 2015; Fig. 1). The rift formation is related to the taphrogenic process that separated the Baltic and Laurentia plates of East Gondwana in the late Brasiliano/Panafrican Orogeny (Bond et al., 1984; Lieberman, 1997; Oliveira and Mohriak, 2003).

Potential field methods have been applied in several studies of rift basins, especially to determine the geometry and thickness, and to identify structures that may be associated with mineral resources. One example is the Mesozoic basins of the Brazilian continental margin, which are leading producers of hydrocarbons in Brazil (Matos, 1992; De Castro, 2011). Early Paleozoic continental rifts can also be economically important due to their association with multiple magmatic events that may occur concurrently or after rifting began, such as Iron Oxide-Copper-Gold (IOCG) deposits reported in the Jaibaras Rift (Paim and Fonseca, 2004; Parente et al., 2004, 2011; Santos et al., 2013).

Ambiguity of solutions, heterogeneity of sources and semi-infinite homogeneous bodies with weak potential field signatures are the main limitations of potential methods (Blakely, 1996;

* Corresponding author. Geological Survey of Brazil, Rua Goiás, 312, CEP 64001-570 Teresina, Brazil.
E-mail address: nilo.pedrosa@cprm.gov.br (N.C. Pedrosa Jr.).

http://dx.doi.org/10.1016/j.jsames.2016.12.012
0895-9811/

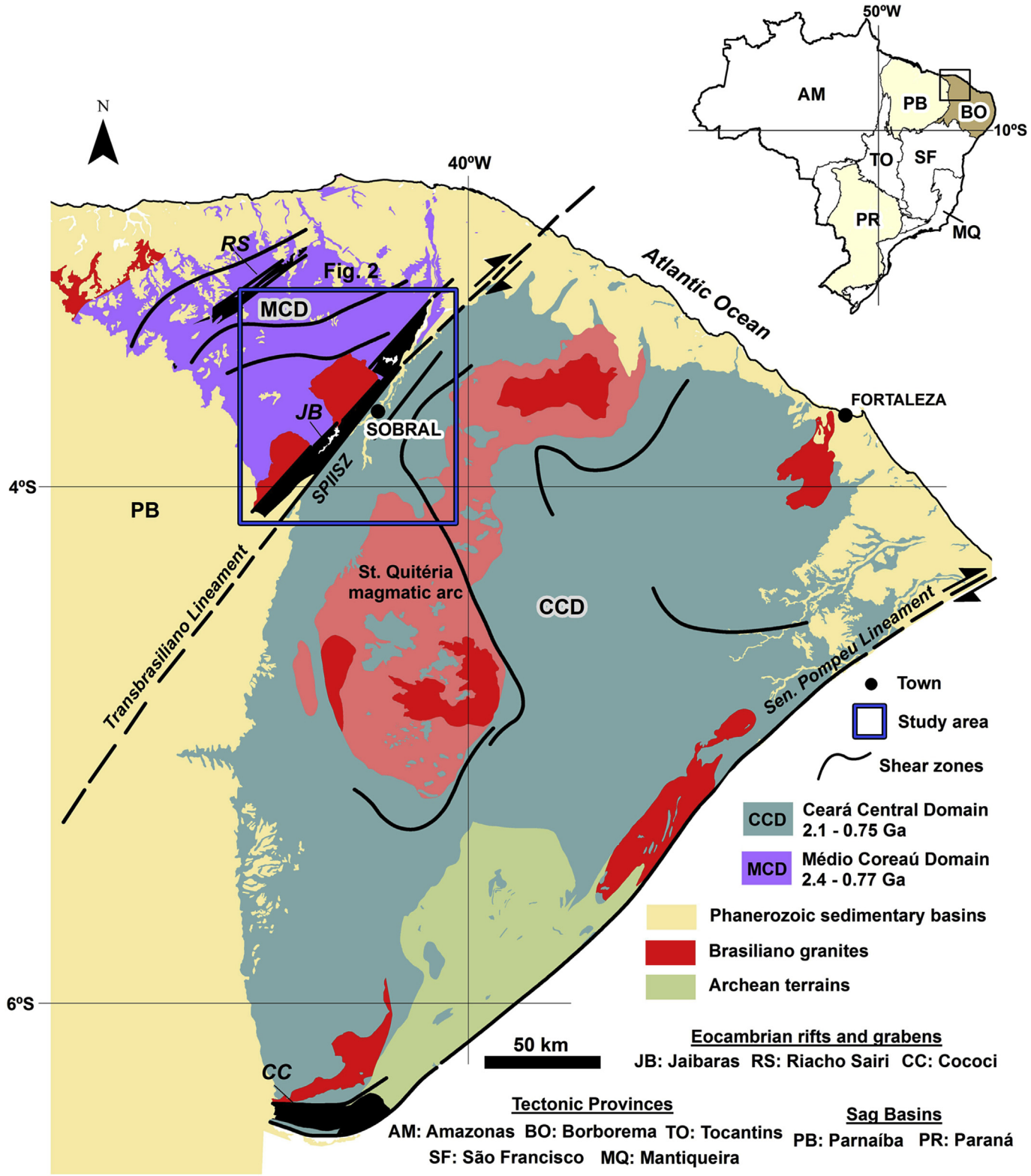

Fig. 1. Simplified geological map of the northern portion of the Borborema Province - Médio Coreaú and Ceará Central domains showing the main tectonic domains and major Brasiliano shear zones. SPIISZ: Sobral-Pedro II Shear Zone (Modified from Cavalcante et al., 2003; Arthaud et al., 2008; Santos et al., 2008).

De Castro, 2011; Saltus and Blakely, 2011). Average density estimates of the outcropping rocks, information from other geophysical methods and boreholes were used to reduce ambiguity. Recently, Pedrosa et al. (2015) discussed and interpreted the gammaspectrometric, magnetic and gravity signatures in the Jaibaras Rift region. Geophysical products generated by the authors show regional structures with major NE-SW and E-W trending lineaments in MCD and NE-SW in CCD (Figs. 1 and 2). A regional 2D

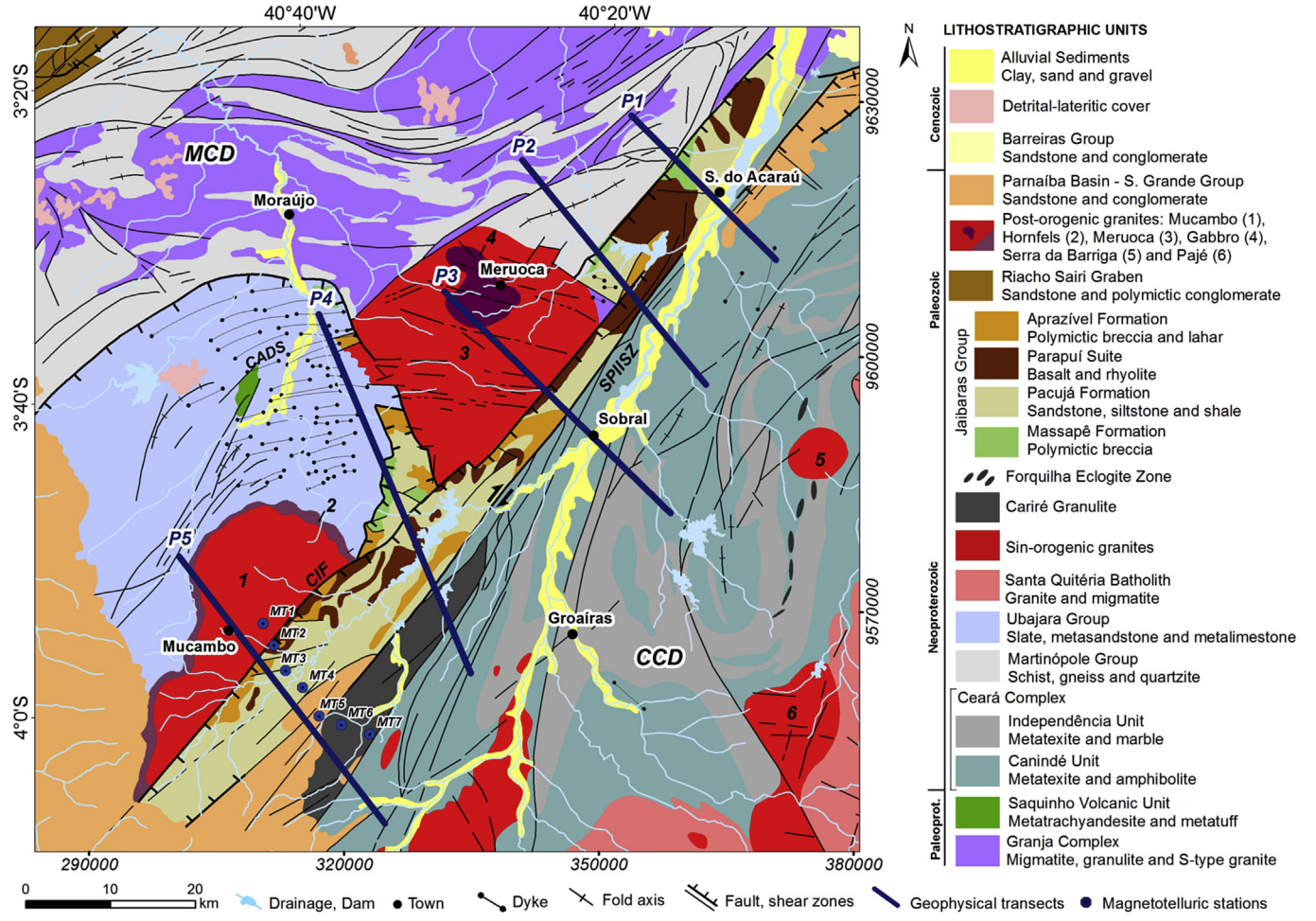

Fig. 2. Geological map of the structural framework of the Jaibaras Basin. Structural domains: MCD - Médio Coreaú; CCD - Ceará Central. SPIISZ - Sobral-Pedro II Shear Zone; CIF – Café-Ipueiras Fault; CADS - Coreaú-Aroeiras Dike Swarm. (Modified from Cavalcante et al., 2003) (Scale: 1:500.000); Santos et al., 2002, 2008; Amaral, 2010; Pedrosa et al., 2015).

forward gravity modeling along a profile perpendicular to the axis of the rift showed that a denser block that extends to the middle crust, whose edge faults calculated depth solutions converge to a semi-graben type structure, characterizes the rift region.

This paper reports on the 2D joint modeling of magnetic and gravity data from five profiles across the main axis of the Jaibaras Rift (Fig. 2), and presents new magnetotelluric data. The main objective of this research is to determine the geometry, depth and thickness of the Jaibaras Rift and its structural framework, using 2D joint modeling of magnetic and gravity data. We also propose a geodynamic model for the Jaibaras Rift.

2. Geological context and the Jaibaras Rift

The Jaibaras Rift (Fig. 2) is of Neoproterozoic-Cambro-Ordovician age and occurs in Precambrian terrains of the Borborema Province. It is located on the boundary between two distinct crustal domains: Ceará Central (CCD) and Médio Coreaú (MCD). The CCD, in the southeastern portion of the area, comprises medium-to high-grade metamorphic rocks, which are part of the Ceará Group and the Tamboril-Santa Quitéria complex. Neoproterozoic supracrustal sequences and their Archean-Paleoproterozoic basement represent the former. The latter is an extensive granite-migmatite complex formed in a continental magmatic arc (Fetter et al., 2003), as well as syn-, late- and post-tectonic granite intrusions. The MCD, limited to the southeast by the SPIISZ (Fig. 2), consists of gneiss and granulite basement rocks of the Paleoproterozoic Granja Complex, schists, gneisses and quartzites of the Neoproterozoic Martinópole Group, low-grade pelites, psammites and carbonate rocks of the Neoproterozoic Ubajara Group, as well as granite and gabbro intrusions (Meruoca and Mucambo) and volcanic and sedimentary rocks of Eopaleozoic basins, such as the Jaibaras Rift and the Jaguarapi Graben (Fig. 2). The Coreaú-Aroeiras dike swarm (CADS in Fig. 2) consists of N80°E to E-W trending vertical dacite and rhyolite dikes, eventually displaying xenoliths of mafic rocks.

The Jaibaras Basin (Fig. 2) is made of two sequences, Alfa Inferior sequence (Ediacaran-Cambrian) represented by the Massapê, Pacujá and Parapuí formations, and Alfa Superior sequence (Cambro-Ordovician), including part of the Parapuí Formation and the Aprazível Formation (Parente et al., 2004). According to Oliveira and Mohriak (2003), the end of the deposition is marked by the beginning of Eosilurian (~440 Ma) sedimentation in the Parnaíba Basin. The Meruoca Granite, dated at 523 ± 9 Ma (Archanjo et al., 2009) and 541 ± 9 Ma (Santos et al., 2013), and the Mucambo Granite (532 ± 9 Ma, Fetter, 1999; Santos, 1999), intrude both the Alfa Inferior and Superior sequences (Parente et al., 2004). From bottom to top the Jaibaras Group comprises the following formations: a) Massapê Formation, consisting of polymict conglomerate with arkosean matrix. The angular and subangular shape of the clasts suggests proximal sources to the deposition area. The clasts are composed of basement and Ubajara Group rocks (Mello, 1978; Costa et al., 1979); b) Pacujá Formation, consisting of micaceous

arkose, shales and subordinate greywacke and conglomerate layers. The rocks are banded due to alternating fine-grained micaceous sandstone and arkose, sometimes including greywacke layers (Gorayeb et al., 1988; Quadros et al., 1994); c) Parapuí Formation (Costa et al., 1973), consisting of a complex suite of bimodal magmatic rocks, including extensive lava flows, pyroclastic rocks and sub volcanic dikes and sills. The formation is cut by the Eopaleozoic Meruoca and Mucambo granites (Fig. 2), the latter bearing partially assimilated andesite xenoliths (Gorayeb et al., 1988; Almeida, 1998); d) Aprazível Formation, ocurring along rift margin faults and steep reliefs, discordantly covering the older formations (Costa et al., 1979). The main rocks of this formation are polymictic conglomerates with clasts of the Massapê, Pacujá and Parapuí formations and basement rocks.

The rift evolution is revealed partly by the stratigraphic sequences that crop out on the rift edges or that were drilled for exploration wells (Oliveira and Mohriak, 2003). Typical proto rift generation is proposed for the basin due to its formation by brittle reactivation processes along Precambrian crustal weakness zones. The rift development is also constrained by four magmatic events related to continental rifting, separated temporally and spatially (Oliveira, 2001). The Coreaú-Aroeiras dike swarm (Fig. 2), of apparent Ediacaran age, is associated with the initial opening stage of the rift. Rb-Sr geochronological data from the dykes indicate ages of 605 ± 31 Ma (Brito Neves et al., 1978), 580 ± 30 Ma (Novais et al., 1979) and 562 ± 10 Ma (Tavares et al., 1990). In the Cambrian, sedimentation was accompanied by mafic magmatism, represented by the rocks of the Parapuí Formation. Parapuí volcanic rock samples were dated at 502 ± 8 Ma and 478 ± 6 Ma (Novais et al., 1979) and 469 ± 13 Ma (Mizusaki and Saracchini, 1990) by the K-Ar method, while the reported U-Pb zircon age is 535.6 ± 8.5 Ma (Garcia et al., 2010). Passive intrusion of the Mucambo and Meruoca plutons (Fig. 2) followed sedimentation and volcanism.

3. Geophysical data

3.1. Aeromagnetic data

Aeromagnetic data (Fig. 3a) were provided by the Geological Survey of Brazil (CPRM), as digital files from the Novo Oriente and Norte do Ceará projects acquired in 2006 and 2008/2009, respectively. Both datasets have the same technical characteristics: 0.1 s sampling interval for the magnetic data, 100 m nominal flight height, N-S flight lines spaced 0.5 km, and E-W tie lines spaced 10 km (AeroGeoPhysica LatinoAmerica, 2006; Prospectors Aerolevantamentos e Sistemas Ltda., 2009). The databases underwent quality control, and problems related to survey flight height and data leveling of the two projects were solved. The magnetic data were interpolated by the bi-directional method - BIGRID (Geosoft, 2014) into a grid of 125 m square cells. The magnetic profiles for 2D modeling were extracted from the magnetic grid, with 100 m sampling space.

The aeromagnetic data were microlevelled. Horizontal, vertical and tilt derivatives of the magnetic anomalies were calculated to enhance specific characteristics of the magnetic signal (Nabighian, 1984; Urquhart, 1988; Minty, 1991; Cordell et al., 1992; Roest et al., 1992).

Fig. 3a shows the magnetic anomalies map of the Jaibaras Rift region, displaying a complex pattern and extensive NE-SW, NW-SE and E-W magnetic alignments. The Médio Coreaú domain (Fig. 3a) shows a pattern of elongated E-W anomalies with NE-SW inflections. The Ceará Central domain (Fig. 3a) is dominated by intermediate magnetic values and relatively quiet magnetic anomaly.

The region can be divided into 11 magnetic domains bounded by the contrasting values of the magnetic anomaly and total gradient amplitude (Pedrosa et al., 2015). The Jaibaras Rift is associated with pronounced negative anomalies of less than 8 km wavelength, and N50°E preferential and E-W subordinate lineaments (Fig. 3a). The high amplitude of the analytic signal and asymmetrical anomalies are related to the volcanic rocks of the Parapuí Formation, which bear potential for Iron Oxide-Copper-Gold (IOCG) deposits (Pedrosa et al., 2015).

3.2. Gravity data

The study area had sparse ground gravity coverage, with approximately 670 measurement stations, concentrated along the main access roads, spaced from 1 to 5 km (Fig. 3b), surveyed by universities and other public institutions in Brazil (Beltrão, 1989; Osako et al., 2011). In addition to these data, 471 new gravity stations were acquired using a digital SCINTREX CG-5 gravimeter. Fig. 3b shows the distribution of previous gravity stations and the newly acquired stations, spaced between 0.5 and 1 km. The gravity data were interpolated using the kriging method (Geosoft, 2014) in 1 km square cells. The gravity and magnetic data were interpolated using different methods, depending on the spatial distribution of each data set (Pedrosa et al., 2015).

The new gravity data were adjusted for tide effects, instrumental drift and latitude, and the free-air and Bouguer anomalies were calculated. The complete Bouguer anomaly map of the Jaibaras Rift area was produced after the data from both previous and newly acquired stations were corrected and integrated. Regional and residual components of the gravity field were separated using a regional-residual separation filter, based on the Gaussian distribution of gravity data in relation to its depth. The filter is a mathematical operator that acts as low-pass of chosen signal frequencies based on the power spectrum in the wave number domain. The standard deviation of the Gaussian function used was 0.04 rad/km, representing the approximate wavelength cutoff of 25 km (Pedrosa et al., 2015). The residual anomalies map highlights the gravity response of shallower crustal heterogeneities (Fig. 3b). The gravity profiles for 2D modeling were extracted from the residual anomaly grid, with a 100 m sampling space.

The residual Bouguer anomaly map comprises negative and positive anomalies from medium to long wavelength (>10 km), and values ranging from −8.9 to 10.6 mGal. Lineaments mostly trend NE-SW, while 2nd order lineaments trend NW-SE and E-W (Fig. 3b). Most of the Jaibaras Rift is characterized by rounded positive gravity anomalies, with wavelength shorter than 10 km. This positive signature results from the significant volume of magmatic rocks of the Parapuí Formation, especially in the northern part of the rift. The strong contribution of these rocks to the local gravity field partially masks the gravity response of the sedimentary rocks of the Jaibaras Rift. This problem was minimized by the joint modeling of magnetic and gravity data.

3.3. Magnetotelluric data

The magnetotelluric (MT) and transient electromagnetic (TDEM) data were acquired in the southern portion of the Jaibaras Rift to support the joint 2D gravity and magnetic forward modeling and reduce ambiguity, increasing the number of physical parameters observed in the region. Magnetotelluric data were recorded at 7 sites spaced ca. 3.5 km in a 25-km long NW-SE profile across the Jaibaras rift, approximately parallel to profile 5 (P5 in Fig. 2).

Broadband data were acquired in a single station configuration using Metronix ADU-07 equipment, with horizontal telluric fields acquired with non-polarized lead chloride electrodes (PbCl) in a cross configuration with 100 m length and three components of the magnetic field acquired with high-sensitivity induction coils

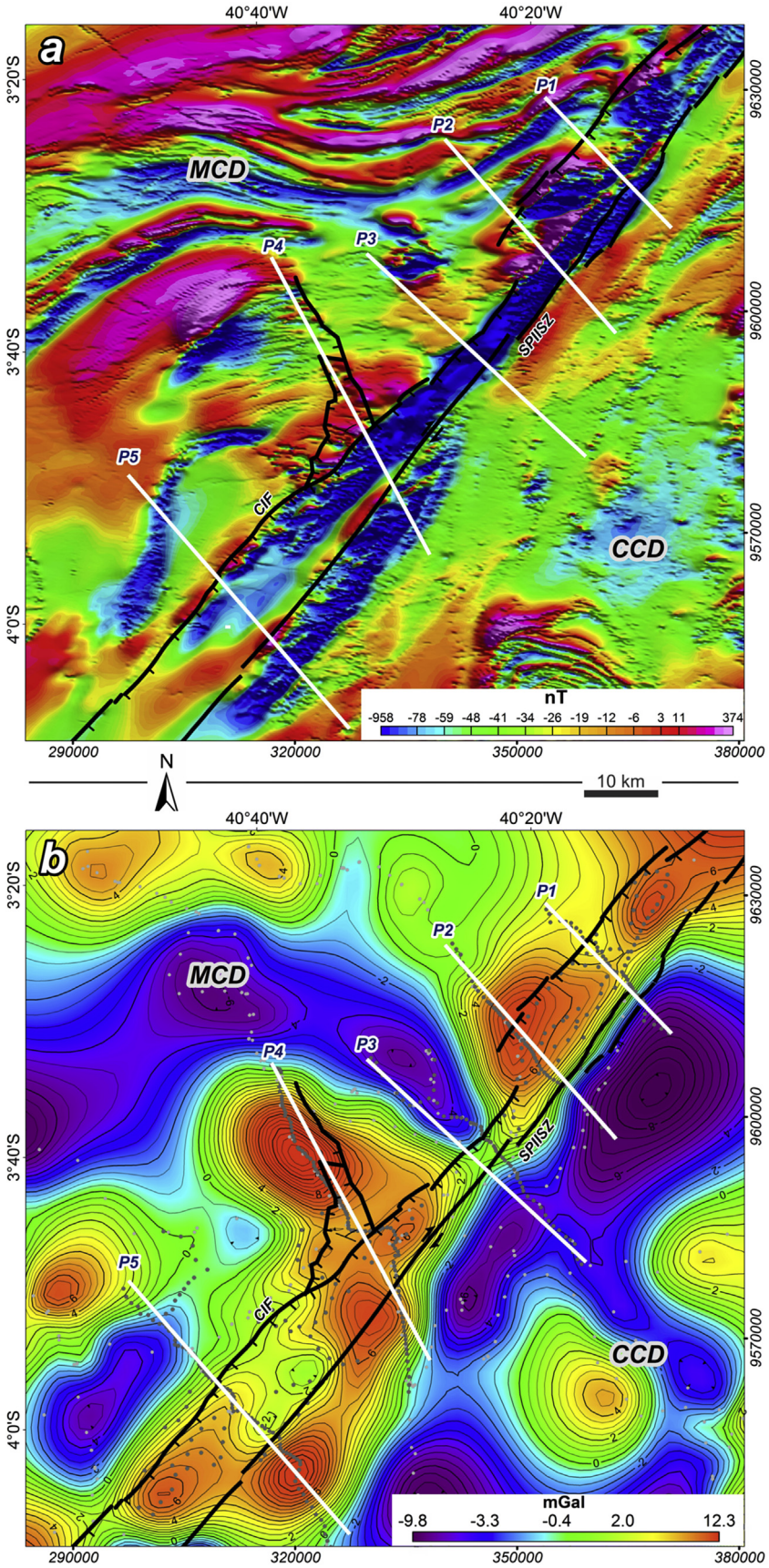

Fig. 3. Magnetic (a) and residual Bouguer gravity (b) anomaly maps of the structural framework of the Jaibaras Rift (adapted from Pedrosa et al., 2015). The main border faults of the rift are represented by black lines, while the geophysical profiles (P1–P5) are represented by white lines. The white and gray dots represent the previous and newly acquired gravity stations, respectively. Structural domains: MCD - Médio Coreaú; CCD - Ceará Central. SPIISZ - Sobral-Pedro II Shear Zone; CIF – Café-Ipueiras Fault.

spaced 3–5 m. The directions used are to the magnetic north, Hx and Ex; and east Hy, and Ey; and to the center of the Earth, Hz. The preprocessing of the data consisted of quality control analysis to remove spurious data from the time series of each component of the electric and magnetic fields (Ex, Ey, Hx, Hy) for each acquired station. This processing was performed using the Mapros software of Metronix.

The TDEM electromagnetic survey used a 100 m square loop to correct the "static shift" effect of the electric field, i.e., the displacement of the apparent resistivity of the Ex and Ey fields due to galvanic currents occurring near the surface that influence the magnetotelluric measurements (Simpson and Bahr, 2005). All acquired MT data were corrected for this effect, and then were followed by inversion procedures.

1D magnetotelluric inverse models were created with three and four layers with different thickness and resistivity values for each of the layers for the 7 stations. The rms misfit between the observed and calculated data by the Ocamm inversion (Constable et al., 1987) is lower than 10%. The geo-electrical strike of 45°Az, corresponding to the tectonic structure of the rift framework, was incorporated to the data. The 2D resistivity model for the southern portion of the Jaibaras Rift (Fig. 4) was generated from the Ocamm inversion algorithm (De Groot-Hedlin and Constable, 1990). The joint inversion procedure for magnetotelluric data was performed with the TE (transverse electric) and TM (transverse magnetic) modes by softness link. The model was generated after 30 iterations, with rms error of 4.08.

4. 2D Euler deconvolution

Euler depth solutions were computed for the magnetic and gravity anomalies (Thompson, 1982; Reid et al., 1990). Euler solutions were generated using structural indices of 0 and 1 for the five geophysical profiles across the Jaibaras Rift (Fig. 3). These indices were used in order to obtaining more linear Euler solutions, possibly estar associated with geological features such as contact, step, sill, dyke and ribbon (Reid et al., 1990). The results show Euler solutions clouds ranging between 0 and 5 km depth. In general, these clouds display very consistent variations along the structural framework of the Jaibaras Rift, showing the complexity of the rift geometry and even the interfering sources associated with the basement rocks and volcanic sequences.

For example, a more detailed analysis of profile 2 (P2, Fig. 6) shows that the Jaibaras Rift boundaries are very well marked by the Euler solutions, specifically solutions generated from the gravity data using a SI of 1, approximately between 15 and 25 km, marking the northwestern and southeastern boundaries, respectively. The magnetic data solutions are shallower and are interpreted to reflect the contact between the sedimentary and volcanic rocks in the rift and/or dykes. The residual gravity anomaly depth solutions display strong correlation to the rift boundary faults and the internal geometry, and a well-developed graben-form structure. The contact between the rift and the basement along P2 can be delineated at the maximum depth of 2 km.

5. 2D magnetic-gravity joint modeling

The joint 2D forward modeling of magnetic and gravity data was performed using the GM-SYS platform (GM-SYS, 2004) of the Oasis Montaj™ package from Geosoft, based on the algorithms developed by Talwani et al. (1959), Talwani and Heirtzler (1964) and Won and Bevis (1987). The magnetic and gravity modeling can be performed by iterative methods or automated techniques using data inversion procedure (Marquardt, 1963). The user defines the location and depth of one or more interfaces separating geological bodies, each with specific densities and magnetic susceptibilities. The calculated values of the magnetic and gravity anomalies from the model bodies are compared to the observed anomalies, and adjustments are made to get the best match between the observed and calculated anomalies. The joint modeling aims to reduce the ambiguity of solutions inherent to potential field methods, as well as information from the magnetotelluric model and estimated

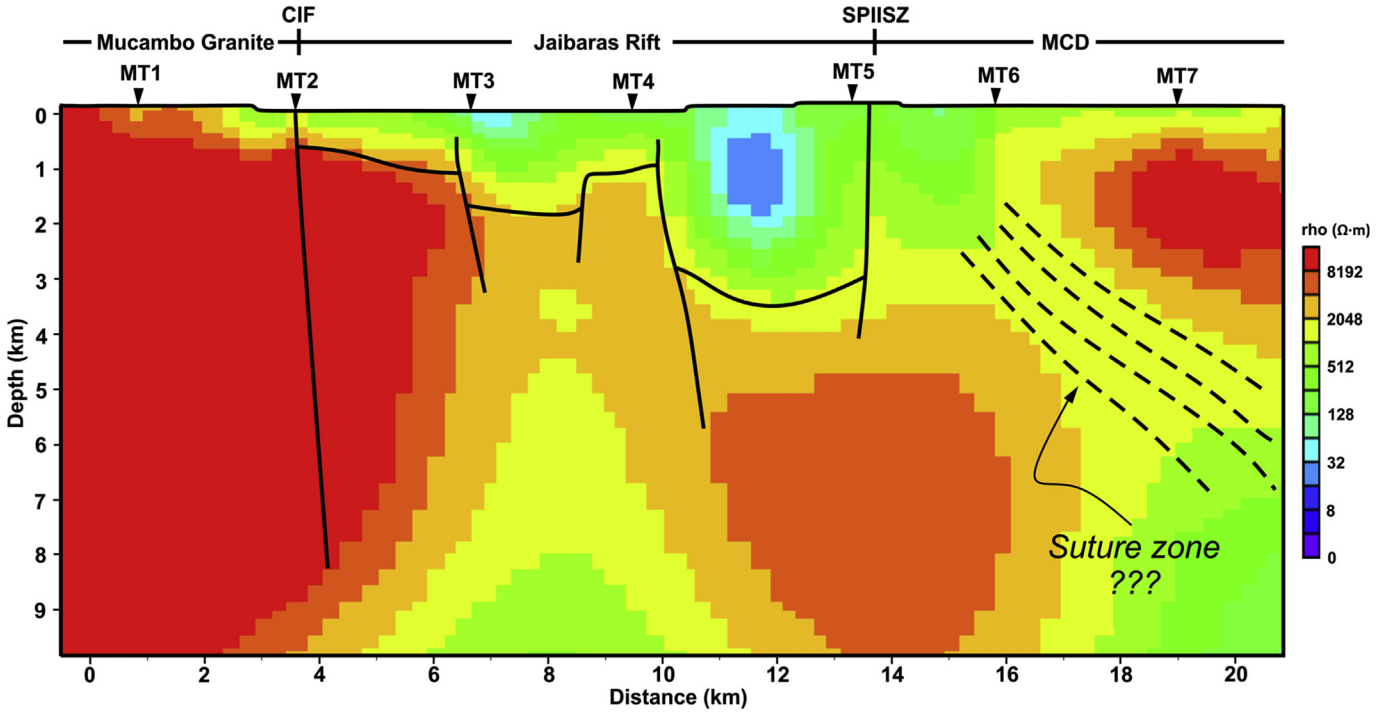

Fig. 4. Two-dimensional interpreted resistivity model of the southern portion of the Jaibaras Rift. SPIISZ: Sobral-Pedro II Shear Zone; CIF: Cafe-Ipueiras Fault.

depths from 2D Euler deconvolution.

Density measurements were conducted on the rocks that crop out in the rift region, so the values could be included in the gravity forward modeling. The average densities of the sedimentary rocks of Massapê, Pacujá and Aprazível formations ranged from 2500 to 2650 kg/m^3, while the densities of the volcanic rocks of the Parapuí Formation are higher and range from 2850 to 2900 kg/m^3. The gneisses and migmatites of the Granja Complex have average values of 2760 kg/m^3 and the metasedimentary rocks of the Martinópole and Ubajara groups have average densities of 2650 and 2600 kg/m^3, respectively. The densities of the supracrustal rocks of the Ceará Group range from 2650 to 2730 kg/m^3. The densities of the Meruoca and Mucambo granites are about 2600 kg/m^3, and gabbroic rocks, 2850 kg/m^3.

6. Interpretation

According to Pedrosa et al. (2015), the Moho interface is smooth with a NW to SE dip, with a thickening crust in the CCD region (Figs. 1 and 2). A gentle upward bulge of the upper mantle marks the rift area; the boundaries between the lower-middle and middle-upper crusts are around 23 km and 12 km, respectively. 2D forward gravity models were determined by separating blocks of different magnetic susceptibilities and densities in the upper crust, with the contacts between the main geological units associated with shear zones or vertical and sub vertical faults (Pedrosa et al., 2015).

6.1. Magnetotelluric data analysis

The inverted 2D magnetotelluric section (Fig. 4) has resistivity values ranging from about 30 to 8000 Ω m, represented by cold and warm colors, respectively, for a 10 km investigation depth. The geological units of the Jaibaras Rift are marked by lower resistivity values (30–200 Ω m), and are in contact with the basement rocks at a maximum depth of 3 km (depocenter; Fig. 4). The Mucambo Granite is highly resistive and the Café-Ipueiras border fault (CIF in Fig. 2) is not well defined in the model due to the spacing of the stations and to the parameter smoothest adopted in the inversions. Therefore, its interpretation is based on the geological mapping data.

The resistivity of CCD ranges between 1000 and 8000 Ω m (Fig. 4); the Cariré granulites are exposed in this area. Some discontinuities/faults are interpreted in the model (Fig. 4) based on resistivity variation laterally and in depth. A lower anomalous resistivity zone (lighter yellow zone) is highlighted, with an approximate 25°SE dip (Fig. 4); this feature is interpreted to be associated with the inferred suture zone mentioned in previous studies (Fetter et al., 2003; Padilha et al., 2014).

6.2. Geophysical models analysis

The extension of the five magnetic and gravity profiles range approximately from 25 to 50 km, trending NW-SE, transverse to the main axis of the Jaibaras Rift (Fig. 2). The objective of the joint modeling study is to establish the geophysical configuration of the shallower crustal levels (Upper Crust: $\leq$ 5 km) and the Jaibaras Rift. The models indicate the geometry and heterogeneity of the geological assemblages within the rift, as well as constraining the major lithostratigraphic units in the border region of the Médio Coreaú and Ceará Central domains. The initial models were guided by available a priori information, such as geological mapping (Cavalcante et al., 2003), magnetotelluric data (Fig. 4), 2D Euler deconvolution, density of rock samples, and regional studies in the Parnaíba Basin that identified features associated with grabens or rifts using seismic reflection and refraction, gravity and magnetotelluric methods (Oliveira and Mohriak, 2003; Conceição et al., 2009; Soares et al., 2010; Osako et al., 2011; De Castro et al., 2014, 2016; Daly et al., 2014; Padilha et al., 2014).

The magnetic and gravity forward models with the observed and calculated anomalies, and the respective geological models of blocks for a depth of up to 5 km are shown in Figs. 5–9. The crustal domain, the geological units, the rock type and gravity and magnetic properties of each block are shown in Table 1. The data fitting errors between the calculated and observed values for the five profiles were given by the method of least squares, and ranged from 18.12% to 24.27% for the magnetic data, and from 0.13% to 0.18% for the gravity data, shown in each section. The fitting of the magnetic data is poorer compared to gravity data, which can be explained by the more complex behavior of the magnetic field vector (Ramadass et al., 2006; Backé et al., 2010; De Castro, 2011). Remnant magnetization was not considered due to lack of information concerning this physical property in the Jaibaras Rift region (Fig. 3).

6.3. Geological models

The geological models for the five transects to the main axis of the Jaibaras Rift are shown in Fig. 10. The portion of the upper crust below the Jaibaras Rift illustrates a heterogeneous Paleoproterozoic basement, marked by denser rocks and more disturbed magnetic anomalies correlated to orthogneiss with mafic and felsic dikes related to the Parapuí Formation of the Jaibaras Group (2 in Fig. 10). This crustal segment is separated by important geological and structural discontinuities that controlled the tectonic evolution of the Jaibaras Rift (SPIISZ and CIF in Figs. 2 and 10). The crystalline basement of the MCD consists of orthogneiss and granulites of the Granja Complex, characterized by higher densities and strong magnetic response (1 in Fig. 10). On the other hand, the Paleoproterozoic basement of the CCD includes more homogeneous and less dense orthogneiss with less intense magnetic response (3 in Fig. 10).

The profiles/transects were analyzed separately due to striking lithological variation and heterogeneity of the geological units observed along the structural framework of the Jaibaras Rift.

In the first 7 km of P1 (Fig. 10), gneiss and migmatite of the Granja Complex and supracrustal sequences of the Martinópole Group crop out, the latter apparently not going deeper than 3 km. Between 7 km and 17.5 km, rocks of the Jaibaras Rift crop out. Polymict breccia of the Massapê Formation, basalts and gabbros of the Parapuí Formation are exposed along the boundary faults, and sandstones of the Pacujá Formation are observed in the central part of the rift. The sedimentary rocks of the Jaibaras Rift are approximately 1.7 km thick in the P1 profile area. In the final part, along the SPIISZ (Fig. 2 and P1 in Fig. 10), about 1 km thick sandstones and conglomerates of the Silurian Serra Grande Group of the Parnaíba Basin are exposed. These thickness values are compatible with depths found by Carvalho (2003), using gravity and shallow seismic refraction data. Southeastwards, the Neoproterozoic supracrustal sequences of the Ceará Group (Canindé and Independência units) are represented by metatexite and amphibolite, close to 5 km deep (P1 in Fig. 10).

The first 14 km of P2 (Fig. 10) are characterized by rocks of the Granja Complex (2 km deep) and metasedimentary sequences (gneiss, schist and quartzite) of the Martinópole Group. The rock package of the Martinópole Group is very deformed and controlled by several Brasiliano shear zones, and displays thickness ranging between 0.5 and 3.2 km (Fig. 2 and P2 in Fig. 10). The Jaibaras Rift is recorded between 14 km and 23.5 km of P2. In the northwest, sedimentary rocks are exposed, whereas at the southeast end of the profile Parapuí Formation volcanic rocks crop out along the SPIISZ.

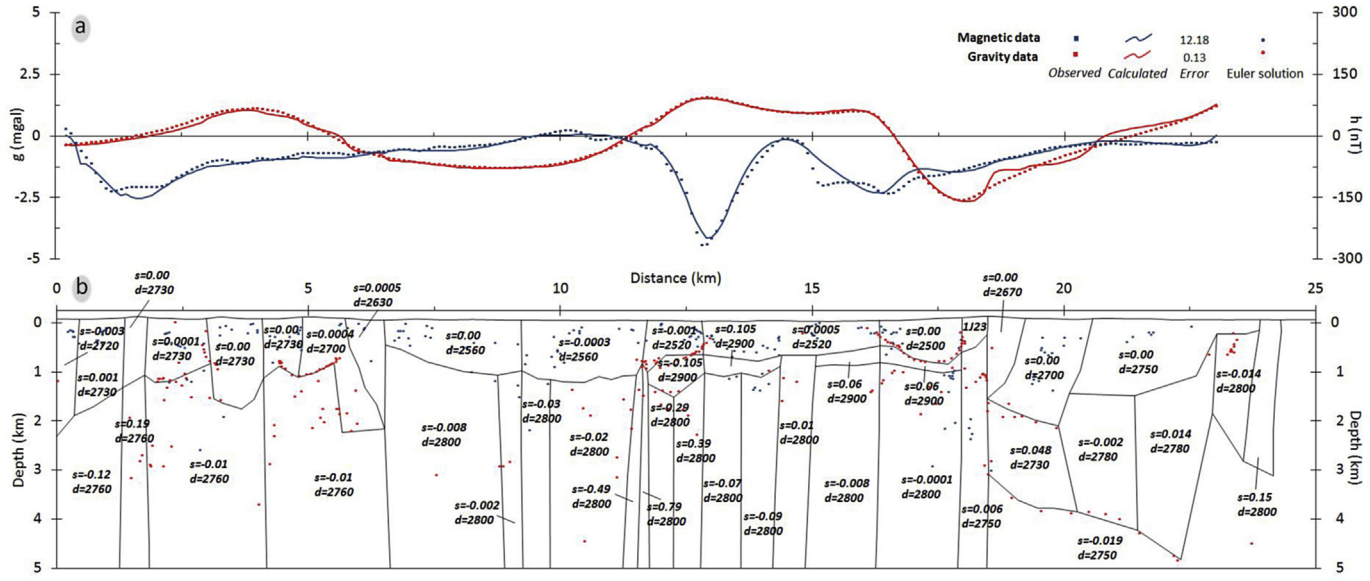

Fig. 5. Observed and calculated magnetic and residual gravity anomalies (a) and the final model of the profile 1 (b). Physical properties and the units of each block are shown in Table 1.

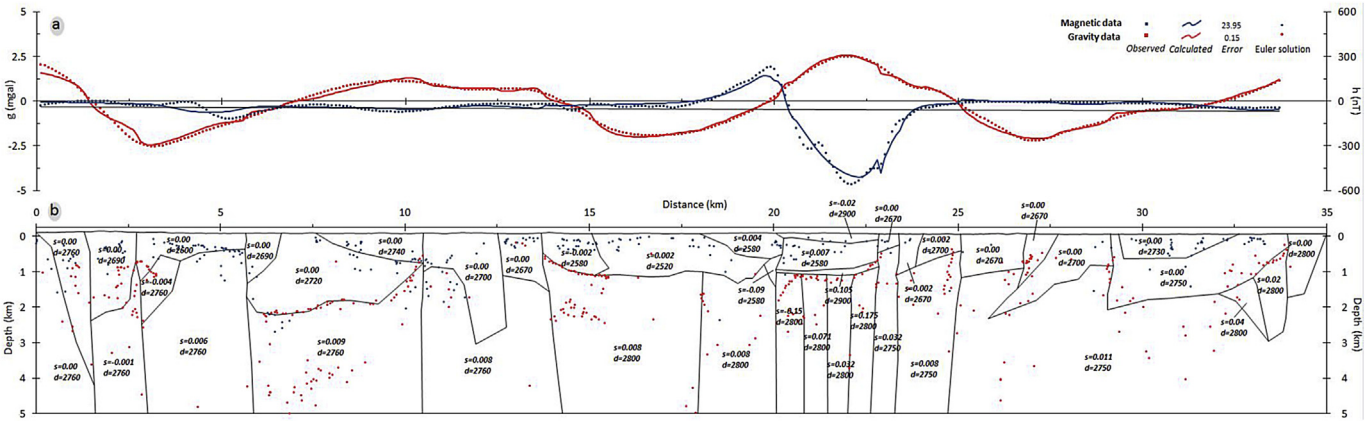

Fig. 6. Observed and calculated magnetic and residual gravity anomalies (a) and the final model of the profile 2 (b). Physical properties and the units of each block are shown in Table 1.

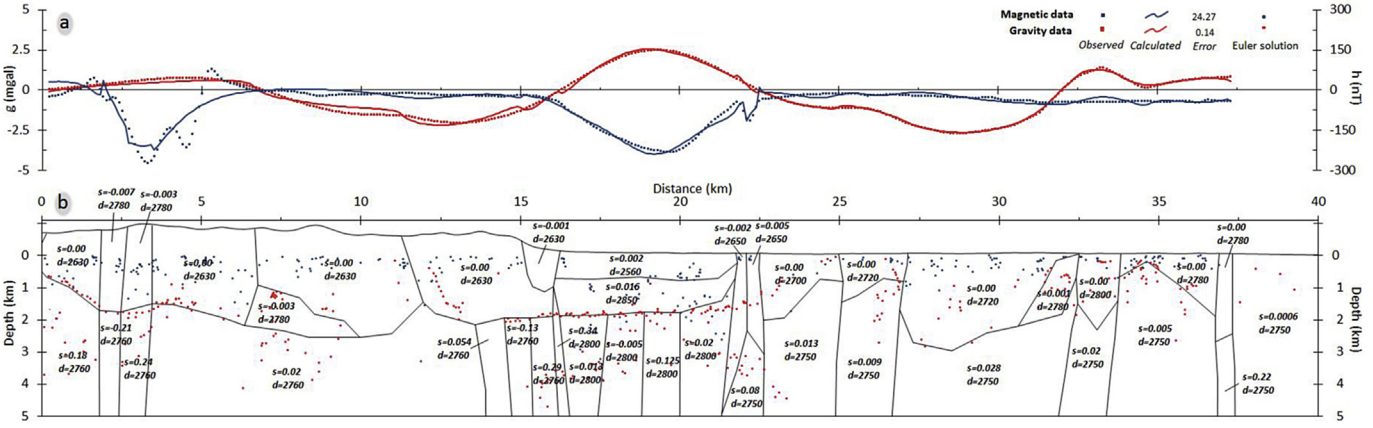

Fig. 7. Observed and calculated magnetic and residual gravity anomalies (a) and result from the joint modeling of geophysical data along profile 3 (b). Physical properties and the geological units of each block are shown in Table 1.

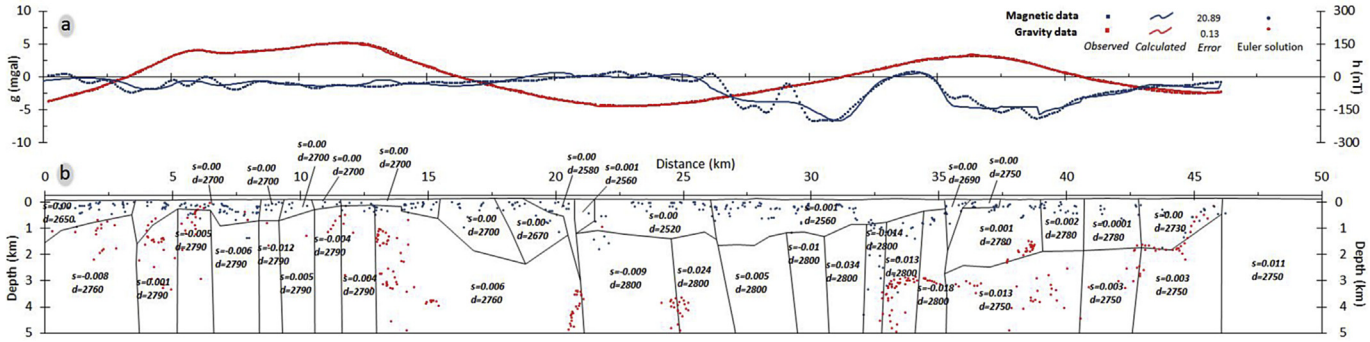

Fig. 8. Observed and calculated magnetic and residual gravity anomalies (a) and the final model of the profile 4 (b). Physical properties and the units of each block are shown in Table 1.

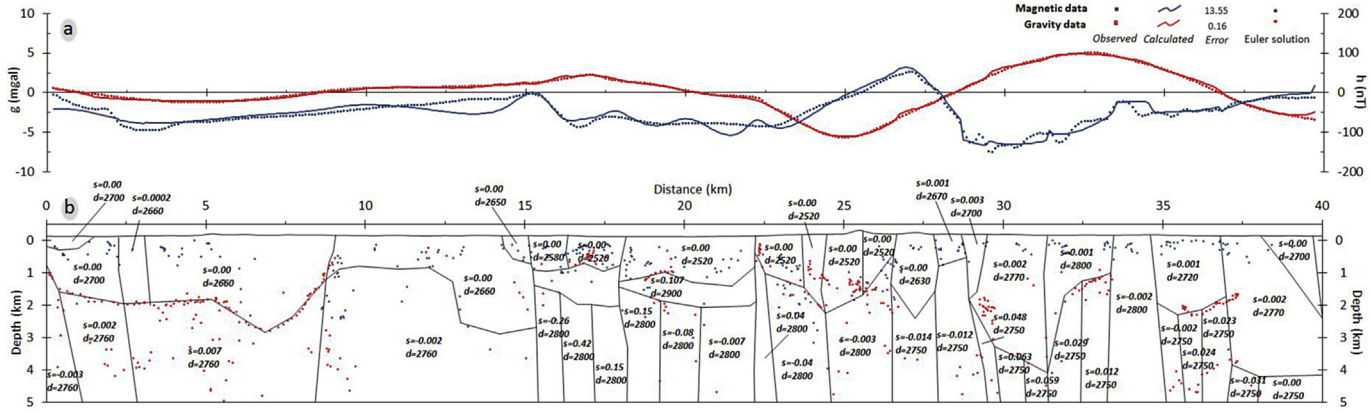

Fig. 9. Observed and calculated magnetic and residual gravity anomalies (a) and the final model of the profile 5 (b). Physical properties and the units of each block are shown in Table 1.

Table 1
Magnetic susceptibility, density and the main geological units used in the joint magnetic-gravity 2D modeling.

Crustal Domain	Geological Unit	Lithology
Ceará Central Domain	Independência Unit	Metatexite, quartzite and metalimestone
	Canindé Unit	Metatexite and schist
		Metabasic rocks and granulite
	Paleoprorerozoic basement	Orthogneiss
Jaibaras Rift	Serra Grande Group	Sandstone and conglomerate
	Massapê and Aprazível formations	Sandstone and Polymictic breccia
	Parapuí Formation	Basalt and rhyolite
	Pacujá Formation	Sandstone and siltstone
	Paleoprorerozoic basement	Orthogneiss with mafic/felsic dykes
Médio Coreaú Domain	Mucambo Granite	Granite and hornfels
	Meruoca Granite	Granite
		Gabbro
	Ubajara Group	Metasandstone, metalimestone and metasiltstone with mafic/felsic dikes
	Martinópole Group	Gneiss, Schist and quartzite
	Granja Complex/Paleoprorerozoic	Orthogneiss, granutite and migmatite

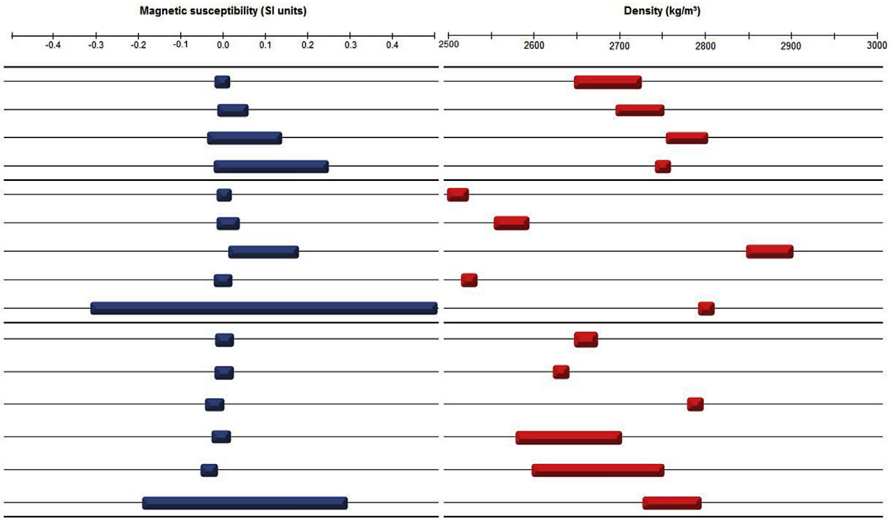

The sedimentary package has a maximum thickness of about 1.6 km, while the basalt flows are less than 0.3 km thick (P2 in Fig. 10). Similar to P1, at the end of P2, rocks of the Canindé and Independência units display sub horizontal dips, and are between 1 and 3 km deep, with some discontinuities associated with indiscriminate shear zones and metabasic rocks (P2 in Fig. 10).

In the initial 16.5 km of P3 (Fig. 10), gabbro and granite of the Meruoca pluton were mapped. This crustal segment has maximum thickness of about 3.8 km. Similar thicknesses have been calculated from gravity and seismic refraction data and modeled by Osako

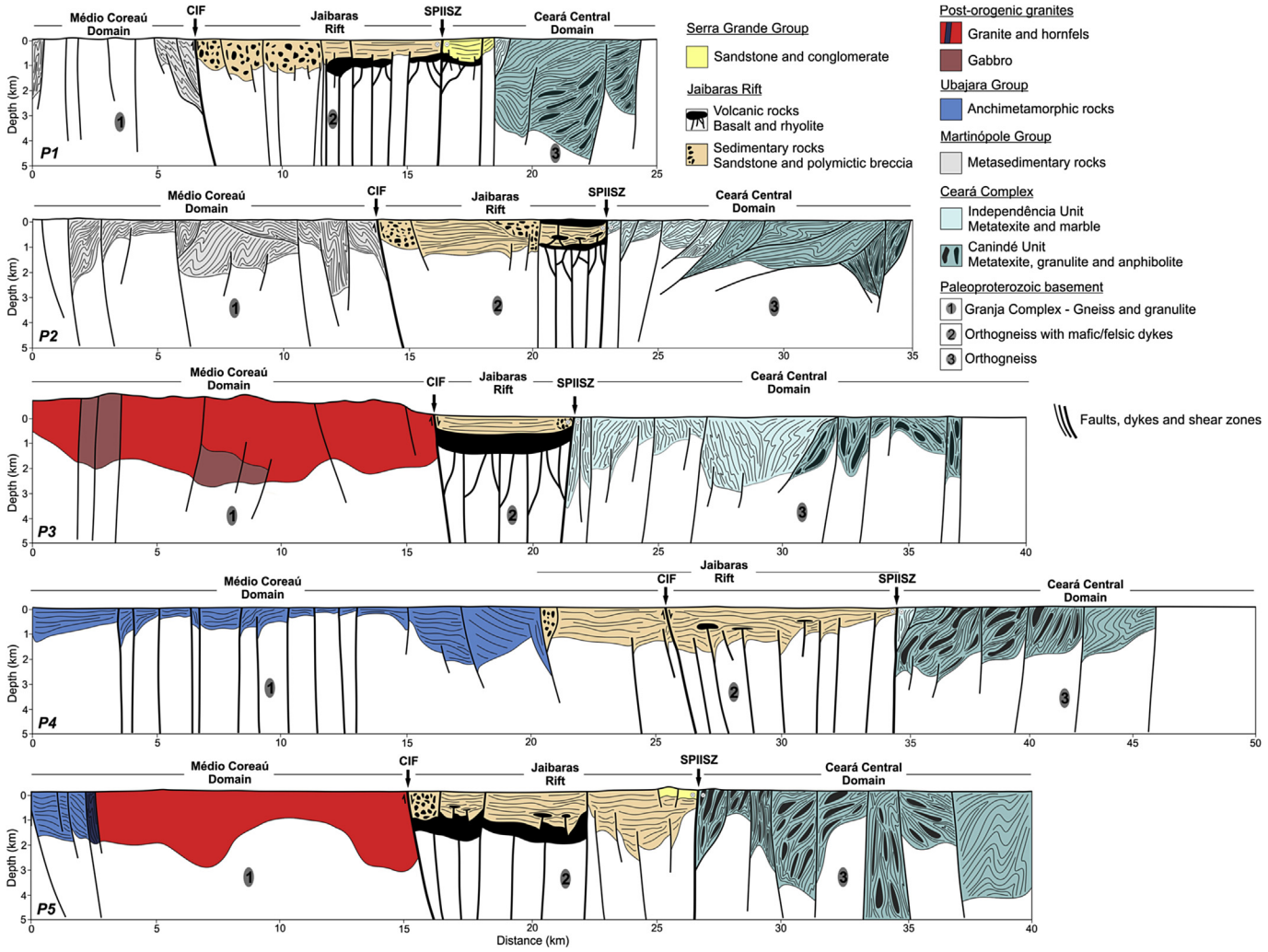

Fig. 10. Geological models obtained from the joint modeling in the five magnetic and gravity profiles for the structural framework region of the Jaibaras Rift.

et al. (2011) and Soares et al. (2010), respectively. P3 crosses the narrowest sector of the Jaibaras Rift, where it is approximately 5 km wide. In this section, outcrops of gabbro dikes of the Parapuí Formation are observed along the boundary faults and a less representative sedimentary sequence of the Pacujá and Aprazível formations. In this area, the thickness of the modeled sedimentary package is about 1 km and the inferred basalt flows extend up to 1.3 km deep (P3 in Fig. 10). From 21.5 km onwards, Neoproterozoic supracrustal rocks of the Ceará Group crop out. In this area, several Brasiliano and indiscriminate shear zones imposed more vertical displacement on the Canindé and Independência units, which are distributed at depths of up to 3 km.

Starting from the west, underformed sandstones and limestones of the Ubajara Group are exposed along 22 km of P4 (Fig. 10), intruded by Coreaú-Aroeiras dikes (CADS in Fig. 2). The anchimetamorphic sequence is thicker along the northwest portion of the rift, about 2.5 km thick, and less than 1.5 km thick in the area where the narrow, vertical to sub vertical dikes are exposed. The rocks of the Jaibaras Rift crop out between 22 km and 34.5 km. The sedimentary package thickness ranges from 1.5 to 2 km, and is represented by an asymmetric set of grabens and horsts. In this area, the rocks of the Parapuí Formation are less abundant on the surface, occurring preferentially as dikes along the Café-Ipueiras fault (P4 in Fig. 10). The southeastern end of P4 is marked by the presence of high-grade metamorphic rocks, including Cariré granulites, metatexite and amphibolite of the Canindé unit, 2–3 km thick, cut by a set of vertical to sub vertical NE-SW shear zones.

At the northwestern end of P5 (Fig. 10), low-grade metamorphic rocks from the Ubajara Group are exposed, cross-cut by thrust faults and shear zones (Fig. 2). The metasedimentary package in this area is about 1.6 km thick. Slate was metamorphosed into hornfels along the contact of the Mucambo granite. Between 3.5 km and 15.5 km of P5, the Mucambo granite is exposed, reaching depths between 1.5 and 3 km. From 15.5 km to 27 km, sedimentary rocks of the Pacujá and Aprazível formations of the Jaibaras Basin and sandstones and conglomerates of the Serra Grande Group of the Parnaíba Basin are exposed. A set of grabens and horsts is interpreted for this area, with maximum thicknesses of about 3 km (P5 in Fig. 10). Thicknesses were estimated in agreement with the analysis of the magnetotelluric data near P5 (Fig. 4). Basaltic flows in subsurface were also inferred, based on the positive magnetic and gravity anomalies. The final portion of the profile is characterized by Cariré granulite and metatexite of the Canindé unit, which are over 5 km deep (P5 in Fig. 10).

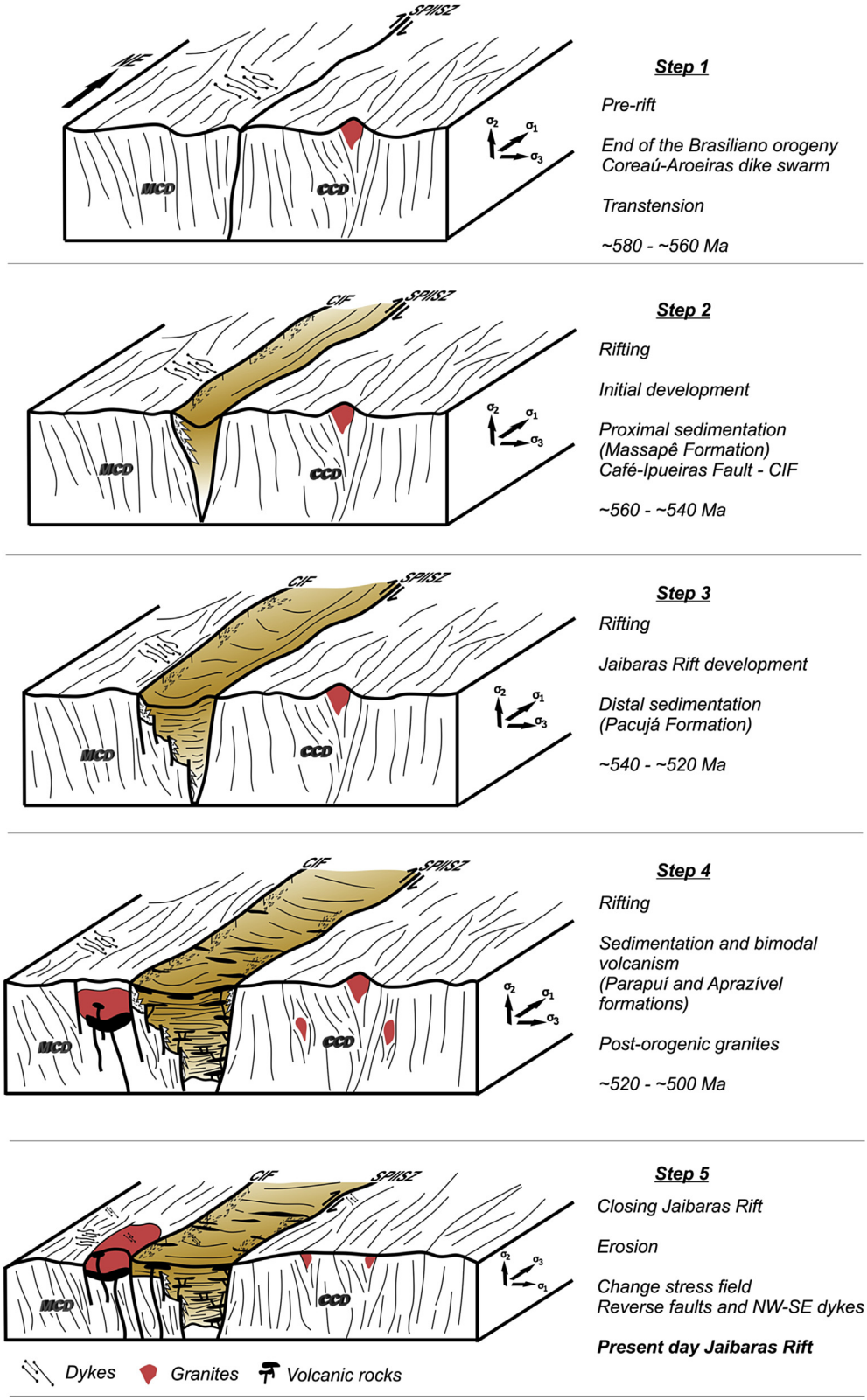

Fig. 11. Geodynamic model for the end of the Neoproterozoic and early Cambrian (post-Brasiliano) showing the evolution and current configuration of the tectonic framework of the Jaibaras Rift.

7. Geodynamic evolution and tectonic considerations

At the end of the Neoproterozoic Brasiliano Orogeny, extensional processes affected the limit between the Médio Coreaú and Ceará Central domains (Fig. 1), in the northern Borborema Province. According to Almeida (1998), the initial stage of the opening of the Jaibaras Rift was due to many maximum efforts, with horizontal σ_1 and σ_3 tensors of E-W and N-S trends, respectively, and vertical σ_2.

These tensors were responsible for the generation and development of the E-W trending extensional fractures where the Coreaú-Aroeiras dike swarm was emplaced (CADS in Fig. 2). These dikes represent the precursor magmatic event of the opening of the Jaibaras Rift (Almeida, 1998; Oliveira, 2001; Step 1 in Fig. 11).

The Early Cambrian is marked by the initial rifting process, with the development of the rift boundary faults, Café-Ipueiras fault at NW and Sobral Pedro II shear zone to SE (Figs. 2 and 11). This stage is characterized by proximal sedimentation, with the deposition of immature sediments represented by polymictic conglomerates of the Massapê Formation (Step 2 in Fig. 11). Further extension of the basin led to sediment deposition in more distal portions of the basin, including sandstones, argillites, siltstones and shales of the Pacujá Formation. The brittle process was also responsible for generating the internal faults in the rift region (Step 3 in Fig. 11).

Fractures propagated down to the base of the Jaibaras Rift, allowing magma of varying composition (basalt and rhyolite) to ascend to the surface and spread out along the major axis of the rift. Lahar-type processes occurred due to the mixing of pyroclastic material with water, which was then deposited in lower energy environments through gravitational mass movements. Breccia and polymictic conglomerates are the products of this process and correspond to the Aprazível Formation. The opening and filling of the rift is complemented with the generation of space allowing the intrusion of granite and gabbro (Step 4 in Fig. 11).

Finally, variations in the stress field of the region created accommodation space in the NW-SE fractures, allowing intrusion of basaltic flows. Similarly striking NW-SE reverse faults are observed in the magnetic maps (Fig. 3a) and in rock exposures documented in the geological map (Pedrosa et al., 2015), particularly in the northern and central parts of the Jaibaras Basin and in the Ubajara Group region (Fig. 2). Later Cambrian and Ordovician times are characterized by tectonic stability. Currently, the basal portion represents the Jaibaras Rift, i.e., post-Cambrian erosional processes resulted in only the “root” of the rift being presently exposed, with average thickness of 1.5 km (Fig. 10 and Step 5 in Fig. 11).

Evidence of fault reactivation has been discussed in some studies, given the recurring earthquakes around the Jaibaras rift and within the Meruoca Granite. These events have approximately E-W trends and are associated with magnetic lineaments or discontinuities of 2nd order (Oliveira et al., 2010; Moura et al., 2014; Pedrosa et al., 2015). Magnetic and gravity data corroborate this interpretation, given the persistent distribution of E-W trending lineaments in the rift region and in the Meruoca Granite (Fig. 3).

Despite of the low lateral resolution of the magnetotelluric data in the region, they clearly establish the limits of the Jaibaras Rift, even if the nature of the Transbrasiliano Lineament (or SPIISZ) is still poorly understood. Lower resistivity anomalies with low-angle and SE dip suggest the existence of suture zone starting at 2.5 km deep (Fig. 4). However, in the shallower part, where the rift is located, the anomalies are narrower and tend to vertical. Probably, this region of the SPIISZ corresponds to the brittle structure that was responsible for opening the basin.

8. Conclusions

Joint 2D modeling of magnetic and gravity data were performed along 5 transects across the Jaibaras Rift, approximately perpendicular to its main NE-SW axis, aiming at a geological model of the internal framework of the rift and of the upper $\leq$5 km of the upper crust. 2D Euler deconvolution data, surface geological information and magnetotelluric cross section in the Southern part of the rift were used to create and constrain geophysical blocks.

The results of the magnetic-gravity joint modeling were satisfactory, and the rms misfit was approximately 20% for the magnetic data and 0.15% for the gravity data. The greater error for the fitting of the magnetic data is attributed to a larger number of shallow magnetic sources with different magnetic susceptibilities and the more complex nature of the rock magnetization and its relation with the geomagnetic field.

The magnetotelluric data corroborate this configuration and show conductive anomalies that are interpreted to be associated with suture between the Ceará Central and Médio Coreaú domains or with weakness zones due to pre-Brasiliano blocks collage.

The Jaibaras Rift displays a very complex internal structure, with a discontinuous sequence of grabens and horsts, and a significant volume of volcanic rocks on the surface and subsurface. The sedimentary packages with volcanic rift sequences have variable thicknesses, from 1 to 3 km (Fig. 10). These rock units are controlled by normal faults that developed from older discontinuities, such as the Transbrasiliano lineament, regionally represented by the Sobral-Pedro II shear zone. The initial rift had a “V” shape, and the evolutionary processes of rifting, erosion and closing after the Cambro-Ordovician caused the NE-SW, E-W and NW-SE trending faults, which continue to undergo reactivation processes.

Future work and more detailed studies, such as modeling and joint inversion of magnetotelluric and gravity data, may improve knowledge on the Jaibaras Rift internal architecture as well as its potential for mineral resources exploration.

Acknowledgments

This article is part of the first author's doctoral dissertation. The research was funded by Transbrasiliano and Instituto Nacional de Ciência e Tecnologia de Estudos Tectônicos projects (FUB/0050.0053151.09.9 Petrobras, and Conselho Nacional de Desenvolvimento Científico e Tecnológico – CNPq - 57.3713/2008-1). The authors are thankful to Instituto Brasileiro de Geografia e Estatística (IBGE) and Serviço Geológico do Brasil (CPRM) for supplying the geophysical data, and to Observatório Nacional (ON) for lending the CG-5 digital Gravimeter for the gravity survey. Thanks are also due to the Laboratório de Geofísica (LGPSR) of Universidade Federal do Ceará for lending the equipment and support in the acquisition of magnetotelluric data. We are grateful to Professor Fernando Santos, Universidade de Lisboa for helping to process the magnetotelluric data. The first author also acknowledges CNPq for the research grant and financial support. R.A.F. thanks CNPq for research grant.

References

AeroGeoPhysica LatinoAmerica, 2006. Relatório final do levantamento e processamento dos dados magnetométricos e gamaespectrométricos. Projeto Aerogeofísico Novo Oriente. Programa Geologia do Brasil, vol. 1. MME, SGMTM, pp. 1–39.

Almeida, A.R., 1998. O magmatismo Parapuí e a evolução geológica da Bacia de Jaibaras. Titular Professor thesis. Universidade Federal do Ceará, p. 125.

Amaral, W.S., 2010. Análise geoquímica, geocronológica e termobarométrica das rochas de alto grau metamórfico, adjacentes ao arco magmático de Santa Quitéria, NW da Província Borborema (Ph.D. thesis). Universidade de Campinas, p. 248.

Archanjo, C.J., Launeau, P., Hollanda, M.H.B.M., Macedo, J.W.P., 2009. Scattering of magnetic fabrics in the Cambrian alkaline granite of Meruoca (Ceará State, northeastern Brazil). Int. J. Earth Sci. 98, 1793–1807.

Arthaud, M.H., Caby, R., Fuck, R.A., Dantas, E.L., Parente, C.V., 2008. Geology of the northern Borborema Province, and its correlations with Nigeria, NW Africa. In: Pankhurst, R.J., Trouw, R.A.J., Brito Neves, B.B., de Witt, M.J. (Eds.), West Gondwana, Pre-Cenozoic Correlations Across the South Atlantic Region, 294. Geological Society, London, Special Publications, pp. 49–67.

Backé, G., Baines, G., Giles, D., Preiss, W., Alesci, A., 2010. Basin geometry and salt diapirs in the Flinders Ranges, South Australia: insights gained from geologically- constrained modelling of potential field data. Mar. Pet. Geol. 27, 650–665.

Beltrão, J.F., 1989. Uma nova abordagem para interpretação de anomalias gravimétricas regionais e residuais aplicada ao estudo da organização crustal – exemplo da região norte do Piauí e noroeste do Ceará (Ph.D. thesis). Universidade Federal do Pará, p. 156.

Blakely, R.J., 1996. Potential Theory in Gravity and Magnetic Applications.

Cambridge University Press, p. 441.
Bond, G.C., Nickeson, P.A., Kominz, M.A., 1984. Breakup of a supercontinent between 625 and 555 Ma: new evidence and implications for continental histories. Earth Planet. Sci. Lett. 70, 325–345.
Brito Neves, B.B., Long, L.L., Kawashita, K., Sial, A.N., Cordani, U.G., Pessoa, R.J.R., 1978. Estudo da geocronologia da faixa costeira pré-cambriana do Nordeste. Unpublished. CNPq, Recife, p. 14.
Carvalho, M.J., 2003. Estruturação do Grupo Serra Grande na região de Santana do Acaraú (CE) e a reativação do Lineamento Sobral-Pedro II: Integração com dados geofísicos (M.S. thesis). Universidade Federal do Rio Grande do Norte, p. 61.
Cavalcante, J.C., Vasconcelos, A.M., et al., 2003. Mapa Geológico do Estado do Ceará – Escala 1:500.000. CDROOM. Ministério das Minas e Energia/Companhia de Pesquisa de Recursos Minerais, Fortaleza, Brasil.
Conceição, M.A.P., Padilha, A.L., Bologna, M.S., 2009. Estudo das estruturas geoelétricas na Província Borborema pelo método magnetotelúrico: Relatório final de projeto de iniciação científica. Conselho Nacional de Desenvolvimento Científico e Tecnológico, p. 36.
Constable, S.C., Parker, R.L., Constable, C.G., 1987. Occam's inversion: a practical algorithm for generating smooth models from electromagnetic sounding data. Geophysics 52, 289–300.
Cordell, L., Phillips, J.D., Godson, R.H., 1992. US Geological Survey Potential Field Geophysical Software Version 2.0. USGS. Open File Report, 92–18.
Costa, M.J., França, J.B., Bacciegga, I.F., Habekost, C.R., Cruz, W.B., 1973. Geologia da Bacia Jaibaras, Ceará, Piauí e Maranhão. Projeto Jaibaras. Recife, Brasil. MME/DNPM Bol. 11, 140.
Costa, M.J., França, J.B., Lins, C.A.C., Bacchiegga, I.F., Habekost, C.R., Cruz, W.B., 1979. Geologia da Bacia de Jaibaras, Ceará, Piauí e Maranhão: Projeto Jaibaras. In: Série Geologia 14, Seção Geologia Básica, vol. 11. MME/DNPM, Brasília, Brasil, p. 106.
Daly, M.C., Andrade, V., Barousse, C.A., Costa, R., McDowell, K., Piggott, N., Poole, A.J., 2014. Brasiliano crustal structure and the tectonic setting of the Parnaíba basin of NE Brazil: results of a deep seismic reflection profile. Tectonics 33. http://dx.doi.org/10.1002/2014TC003632.
De Castro, D.L., 2011. Gravity and magnetic joint modeling of the Potiguar rift basin (NE Brazil): basement control during Neocomian extension and deformation. J. S. Am. Earth Sci. 31, 186–198.
De Castro, D.L., Bezerra, F.H.R., Fuck, R.A., Vidotti, R.M., 2016. Geophysical evidence of pre-sag rifting and post-rifting fault reactivation in the Parnaíba Basin, Brazil. Solid Earth. 7, 529–548.
De Castro, D.L., Fuck, R.A., Phillips, J.D., Vidotti, R.M., Bezerra, F.H.R., Dantas, E.L., 2014. Crustal structure beneath the Paleozoic Parnaíba Basin revealed by airborne gravity and magnetic data, Brazil. Tectonophys. Amst. 614, 128–145.
De Groot-Hedlin, C., Constable, S.C., 1990. Occam's inversion to generate smooth, two-dimensional models from magnetotelluric data. Geophysics 55, 1613–1624.
Fetter, A.H., 1999. U-Pb and Sm-Nd Geochronological Constraints on the Crustal Framework and Geologic History of Ceará State, NW Borborema Province, NE Brazil: Implications for the Assembly of Gondwana (Ph.D. thesis). University of Kansas, USA, p. 164.
Fetter, A.H., Santos, T.J.S., Van Schmus, W.R., Hackspacher, P.C., Brito Neves, B.B., Arthaud, M.H., Nogueira, J.A., Wernick, E., 2003. Evidence for neoproterozoic continental arc magmatism in the Santa Quitéria Batholith of Ceará state, NW Borborema province, NE Brazil: implications for the assembly of west Gondwana. Gondwana Res. 6, 265–273.
Garcia, M.G.M., Parente, C.V., Silva Filho, W.F., Almeida, A.R., 2010. Idade do vulcanismo ácido da Formação Parapuí: implicações na estratigrafia da Bacia Eopaleozóica Jaibaras-CE. In: Presented at the 45th Congresso Brasileiro de Geologia.
Geosoft, 2014. Oasis Montaj How- to Guide. Complete Workflow for Oasis Montaj. Geosoft Incorporated, Toronto, Ontario, Canada, p. 260.
GM-SYS, 2004. Gravity/magnetic Modeling Software: User's Guide Version 4.9. NGA Inc., p. 101
Gorayeb, P.S.S., Abreu, F.A.M., Correa, J.A.M., Moura, C.A.V., 1988. Relações estratigráficas entre o granito Meruoca e a sequência Ubajara-Jaibaras. In: Presented at the 35th Congresso Brasileiro de Geologia.
Lieberman, B.S., 1997. Early Cambrian paleogeography and tectonic history: a biogeography approach. Geology 25, 1039–1042.
Marquardt, D.W., 1963. An algorithm for least squares estimation of nonlinear parameters. J. Soc. Ind. Appl. Math. 11, 431–441.
Matos, R.M.D., 1992. The northeast Brazilian rift system. Tectonics 11 (4), 766–791.
Mello, Z.F., 1978. Evoluções finais do ciclo geotectônico Brasiliano no Nordeste Oriental. In: Presented at the 30th Congresso Brasileiro de Geologia.
Minty, B.R.S., 1991. Simple micro-levelling for aeromagnetic data. Explor. Geophys. 22, 591–592.
Mizusaki, A.M.P., Saracchini, F.E., 1990. Catálogo geral de dados geocronológicos da Petrobrás. Petrobrás/Cenpes, Rio de Janeiro, p. 24 internal report. Unpublished.
Moura, A.C.A., Oliveira, P.H.S., Bezerra, F.H.R., Ferreira, J.M., Fuck, R.A., Nascimento, A.F., 2014. Seismogenic faulting in the Meruoca granite, NE Brazil, consistent with a local weak fracture zone. An. Acad. Bras. Ciências 86 (4), 1631–1639.
Nabighian, M.N., 1984. Toward a three-dimensional automatic interpretation of potential field data via generalized Hilbert transforms: fundamental relations. Geophysics 49, 780–786.
Novais, F.R.G., Brito Neves, B.B., Kawashita, K., 1979. Reconhecimento cronoestratigráfico na região Noroeste do Ceará. In: Presented at the 9th Simpósio de Geologia do Nordeste.
Oliveira, D.C., Mohriak, W.U., 2003. Jaibaras trough: an important element in the early tectonic evolution of the Parnaíba interior sag basin, Northern Brazil. Mar. Pet. Geol. 20, 351–383.
Oliveira, D.C., 2001. Reavaliação da evolução tectono-magmática do Graben de Jaibaras (Nordeste do Brasil). Acta Geol. Hisp. 36 (1/2), 53–95.
Oliveira, P.H.S., Ferreira, J.M., Nascimento, A.F., Bezerra, F.H.R., Soares, J.E., Fuck, R.A., 2010. Estudo da Sismicidade na Região de Sobral-CE, NE do Brasil em 2008. In: Presented at the 4th Simpósio Brasileiro de Geofísica.
Osako, L.S., Castro, D.L., Fuck, R.A., Castro, N.A., Pitombeira, J.P.A., 2011. Contribuição de uma seção gravimétrica transversal ao estudo da estruturação litosférica na porção setentrional da Província Borborema, NE do Brasil. Rev. Bras. Geofísica 29 (2), 309–329.
Padilha, A.L., Vitorello, I., Padua, M.B., Bologna, M.S., 2014. Electromagnetic constraints for subduction zones beneath the northwest Borborema province: evidence for Neoproterozoic island arc-continent collision in northeast Brazil. Geology 42, 91–94.
Paim, P.S.G., Fonseca, M.M., 2004. Setor Meridional da Província Mantiqueira – Bacias do Camaquã e Itajaí. In: Mantesso-Neto, V., Bartorelli, A., Carneiro, C.D.R., Brito Neves, B.B. (Eds.), Geologia do Continente Sul Americano, vol. 29. Evolução da Obra de Fernando Flávio Marques de Almeida, pp. 490–500.
Parente, C.V., Botelho, N.F., Santos, R.V., Garcia, M.G.M., Oliveira, C.G., Verissimo, C.U.V., 2011. Contexto Geológico, Tipológico e Geoquímico Isotópico das Brechas Hidrotermalizadas de Ferro e Cobre tipo IOCG, associadas à Bacia Eo-Paleozóica Jaibaras, da Província Borborema, Brasil. In: Frantz, J.C., Marques, J., Jost, H. (Eds.), Contribuições à Metalogenia do Brasil, vol. 1. Universidade do Rio Grande do Sul, p. 26.
Parente, C.V., Filho, W.F.S., Almeida, A.R., 2004. Bacias do Estágio de Transição do Domínio Setentrional da Província Borborema. In: Mantesso-Neto, V., Bartorelli, A., Carneiro, C.D.R., Brito Neves, B.B. (Eds.), Geologia do Continente Sul Americano, vol. 29. Evolução da Obra de Fernando Flávio Marques de Almeida, pp. 525–536.
Pedrosa Jr., N.C., Vidotti, R.M., Fuck, R.A., Leopoldino Oliveira, K.M., Castelo Branco, R.M.G., 2015. Structural framework of the Jaibaras Rift, Brazil, based on geophysical data. J. S. Am. Earth Sci. 58, 318–334.
Prospectors Aerolevantamentos e Sistemas LTDA, 2009. Relatório final do levantamento e processamento dos dados magnetométricos e gamaespectrométricos. Projeto Aerogeofísico Norte do Ceará. Programa Geologia do Brasil, vol. 1. MME, SGMTM, pp. 1–40.
Quadros, M.L.E.S., Abreu, F.A.M., Gorayeb, P.S.S., 1994. Considerações sobre os ambientes deposicionais das formações Pacujá e Aprazível, Bacia de Jaibaras - NW do Ceará. In: 38th Congresso Brasileiro de Geologia, Expanded Abstracts, pp. 240–242.
Ramadass, G., Ramaprasada Rao, I.B., Himabindu, D., 2006. Crustal configuration of the Dharwar Craton, India, based on joint modeling of regional gravity and magnetic data. J. Asian Earth Sci. 26, 437–448.
Reid, A.B., Allsop, J.M., Granser, H., Millett, A.J., Somerton, I.W., 1990. Magnetic interpretation in three dimensions using Euler deconvolution. Geophysics 55, 80–91.
Roest, W.R., Verhoef, J., Pilkington, M., 1992. Magnetic interpretation using the 3D analytical signal. Geophysics 57 (1), 116–125.
Saltus, R.W., Blakely, R.J., 2011. Unique geologic insights from “non-unique” gravity and magnetic interpretation. Geol. Soc. Am. 21 (12), 4–10.
Santos, R.V., Oliveira, C.G., Parente, C.V., Garcia, M.G.M., Dantas, E.L., 2013. Hydrothermal alteration related to a deep mantle source controlled by a Cambrian intracontinental strike-slip fault: evidence for the Meruoca felsic intrusion associated with the Transbraziliano lineament, northeastern Brazil. J. S. Am. Earth Sci. 43, 33–41.
Santos, T.J.S., 1999. Evolução Tectônica e Geocronológica do Extremo Noroeste da Província Borborema (Ph.D. thesis). IGCE/UNESP, Rio Claro, SP, p. 186.
Santos, T.J.S., Fetter, A.H., Nogueira Neto, J.A., 2008. Correlation of the west margin of the transbrasiliano–kandi lineament in the Borborema province (NE Brazil) and Pharusian Belt (NW Africa). In: Pankhurst, R.J., Trouw, R.A.J., Brito Neves, B.B., Wit, M.J. (Eds.), West Gondwana: Pre-cenozoic Correlations a Cross the South Atlantic Region, vol. 294. Geological Society, Special Publications, pp. 101–119.
Santos, T.J.S., Souza, G.M., Queiroz, H.B., Nogueira Neto, J.A., Parente, C.V., 2002. Tafrogênese estateriana no embasamento paleoproterozóico do NW da Província Borborema: Uma abordagem petrográfica, geoquímica e geocronológica. In: 41st Congresso Brasileiro de Geologia, Extended Abstracts, p. 337.
Schobbenhaus, C., Campos, D.A., Derze, G.R., Asmus, H.E., 1975. Texto explicativo. Folha Goiás SD.22. In: Schobbenhaus, C. (Ed.), Carta Geológica do Brasil Milionésimo. DNPM, Brasília.
Simpson, F., Bahr, K., 2005. Practical Magnetotellurics. Cambridge University Press, p. 254.
Soares, J.E.P., Lima, M.V., Fuck, R.A., Berrocal, J., 2010. Características sísmicas da litosfera da Província Borborema: resultados parciais do experimento de refração sísmica profunda. In: Presented at the 4th Simpósio Brasileiro de Geofísica.
Talwani, M., Heirtzler, J.R., 1964. Computation of magnetic anomalies caused by 2D bodies of arbitrary shape. In: Parks, G.A. (Ed.), Computers in the Mineral Industries, Part 1, Geological Sciences, vol. 9. Stanford University Publications, pp. 464–480.
Talwani, M., Worel, J.L., Landisman, M., 1959. Rapid gravity computations for 2D bodies with application to the Mendocino submarine fracture zone. J. Geophys.

Res. 64, 49–59.
Tavares Jr., S.S., Gorayeb, P.S.S., Lafon, J.M., 1990. Petrografia e geocronologia Rb/Sr do feixe de diques da borda oeste do Granito de Meruoca (CE). In: 36th Congresso Brasileiro de Geologia, Expanded Abstracts, pp. 337–338.
Thompson, D.T., 1982. EULDPH: a new technique for making computer assisted depth estimates from magnetic data. Geophysics 47, 31–37.
Urquhart, T., 1988. Decorrugation of enhanced magnetic field maps - expanded Abstracts and Biographies. In: 58th Annual Meeting, vol. 7. Society of Exploration Geophysicists, pp. 371–372.
Won, I.J., Bevis, M., 1987. Computing the gravitational and magnetic anomalies due to a polygon: algorithms and Fortran subroutines. Geophysics 52, 232–238.